Influence of fiber paths on buckling load of tailored conical shells

Ali-Asghar Naderi [1a], Gholam-Hossein Rahimi [*1] and Mohammad Arefi [2b]

[1] *Mechanical Engineering, Tarbiat Modares University, Jalal Ale Ahmad Highway,*
P.O. Box: 14115-111, Tehran, Iran
[2] *Department of Solid Mechanics, Faculty of Mechanical Engineering,*
University of Kashan, Kashan 87317-51167, Iran

Abstract. The purpose of this paper is to propose a method for evaluation of varying stiffness coefficients of tailored conical shells (TCS). Furthermore, a comparison between buckling loads of these shells under axial load with the different fiber path is performed**.** A circular truncated conical shell subjected to axial compression is taken into account. Three different theoretical path containing geodesic path, constant curvature path and constant angle path has been considered to describe the angle variation along the cone length, along cone generator of a conical shell are offered. In the TCS with the arbitrary fiber path, the thickness and the ply orientation are assumed to be functions of the shell coordinates and influencing stiffness coefficients of the structure. The stiffness coefficients and the buckling loads of shells are calculated basing on classical shells theory (CST) and using finite-element analysis (FEA) software. The obtained results for TCS with arbitrary fiber path, thickness and ply orientation are derived as functions of shell longitudinal coordinate and influencing stiffness coefficients of structures. Furthermore, the buckling loads based on fiber path and ply orientation at the start of tailored fiber get to be different. The extent of difference for tailored fiber with start angle lower than 20 degrees is not significant. The results in this paper show that using tailored fiber placement could be applied for producing conical shells in order to have greater buckling strengths and lower weight. This work demonstrates the use of fiber path definitions for calculated stiffness coefficients and buckling loads of conical shells.

Keywords: composite; fiber path; tailored conical shells; stiffness coefficients; buckling

1. Introduction

Conical shells occur frequently as components of aeronautic, marine and civil engineering structures. Often they are frequently used as transition elements joining cylinders of different diameters. Thus, the design of minimum weight, maximum strength stiffened conical shells under loads has long been of interest to designers. The advent of high strength, light weight, composite materials has resulted in broad use of multi-layered shells. Buckling and loss of stability of

---

∗Corresponding author, Professor, E-mail: rahimi_gh@modares.ac.ir
[a] Ph.D. Student, E-mail: asi1349@yahoo.com
[b] Assistant Professor, E-mail: arefi63@gmail.com; arefi@kashanu.ac.ir

stiffened conical shells is one of the most important and crucial failure phenomena of such structures. It is well known that stability of conical shells has been studied by many researchers with a variety of shell and plate theories (Seide 1956, 1957, Singer 1963, Arbocz 1968, Baruch *et al*. 1970, Tong *et al*. 1992, Tong and Wang 1992). In these researches, the stiffness coefficients of a conical shell are usually assumed to be constant. Unlike an isotropic conical shell, in the case of a shell of laminated composite material the thickness and the material properties vary with the shell coordinates, which ultimately results in coordinate dependence of stiffness coefficients. An exhaustive study of the stiffness functions and their dependence on geometry of the cone has been performed by Baruch *et al*. (1993). Goldfeld and Arbocz (2004) investigated the buckling load of laminated conical shells taking into account the variation of stiffness coefficients along the coordinates using the computer code. The optimization and sensitivity of laminated conical shells to imperfection taking into account the variations of the stiffness coefficients for buckling have been studied by Goldfeld *et al*. (2005) and Goldfeld (2007a, b), respectively. Abdalla *et al*. (2007) considered maximization of the natural frequency of variable stiffness composite panels. The concept of constructing variable-stiffness shells has been extended to truncated conical shell by Blom *et al*. (2008, 2009). Blom *et al*. (2010) presented a method for designing composite plies with varying fiber angles with composite panels.

In this work, three paths definitions for arbitrary conical shells were proposed that can be used to describe the variation of fiber orientation along the length of the cone. These paths will be used for buckling analysis of laminated conical shell. Basing on the work of Goldfeld and Arbocz (2004) and Goldfeld *et al*. (2005) who considered laminated conical shells for the variations of the stiffness coefficients for the geodesic path, this study is an attempt to extend their work to the constant curvature and the constant angle paths for elastically TCS, and the buckling load of shells are calculated.

2. Governing equation

Consider a circular truncated conical shell subjected to axial compression, as shown in Fig. 1, where t denotes the thickness of the shell and the values r_1, and r_2 are radii of the cone at the small and large edges, respectively, α is the semi vertex angle of the cone, and L is the cone length along its generator. We introduce a set of conical coordinate x-θ that it is located on the middle surface, x is measured along the cone's generator starting from the small radius of the shell and θ is the circumferential coordinate. The displacements of the shell's middle surface are denoted by U and V along x and θ direction, respectively and by W along the normal to surface (inward positive) (Tong and Wang 1992).

In this coordinate system, the cone's radius r, which is the perpendicular distance from the axis of revolution at any point, is the length varies linearly following

$$r = r_1 + x\sin\alpha \tag{1}$$

Where, r_1 is the cone's radius at the small edge. In order to design a feasible ply, constructed by laying down multiple paths, general expressions are required for the orientation and curvature of a path contained on the surface of conical structure. For this purpose φ is defined as the angle between the longitudinal surface direction and the tangent to the fiber path. For variable-stiffness laminates, this angle is defined as a function of x. Referring to Fig. 1, we conclude from the geometry of fiber that the fiber orientation is expressed as
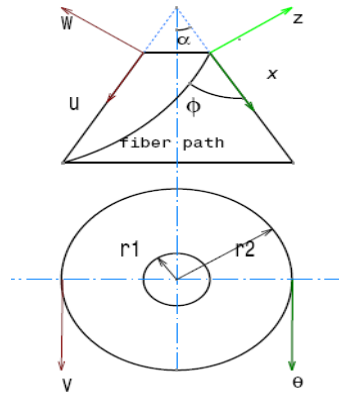
Fig. 1 Coordinate system, the fiber path and the geometrical details of the conical shell
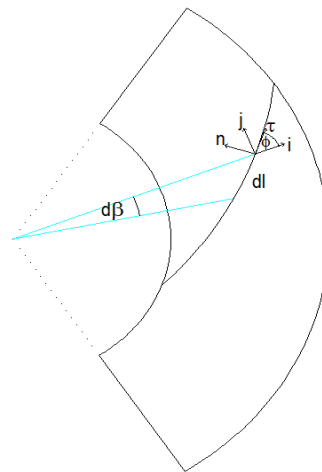
Fig. 2 Flattened configuration of the cone

$$\tan\varphi = \frac{rd\theta}{dx} \qquad (2)$$

The unit tangent vector to the fiber path, $\hat{\tau}$, is

$$\hat{\tau} = \cos\varphi\vec{i} + \sin\varphi\vec{j} \qquad (3)$$

Where, $\vec{i}$ represents the in-plane vector in the longitudinal surface direction of the flattened configuration of the cone (shown in Fig. 2) and $\vec{j}$ represents the in-plane vector normal to the longitudinal surface direction of the flattened configuration of the cone.

There are several formulas for determining the curvature for a curve. The formal definition of curvature is

$$\kappa = \left| \frac{d\hat{\tau}}{dl} \right| = \left| \frac{d\hat{\tau}}{d\varphi} \frac{d\varphi}{dx} \frac{dx}{dl} \right| \tag{4}$$

Where, $\hat{\tau}$ is the unit tangent and l is the arc length. From Eq. (3) it follows by differentiation that

$$\frac{d\hat{\tau}}{d\phi} = -\sin\varphi\vec{i} + \cos\varphi\frac{d\vec{i}}{d\beta}\frac{d\beta}{d\varphi} + \cos\varphi\vec{j} + \sin\varphi\frac{d\vec{j}}{d\beta}\frac{d\beta}{d\varphi} \tag{5}$$

We need expressions for the derivatives of both unit vectors using the geometry of in-plane vectors of the flattened configuration in Fig. 2.

$$\frac{d\vec{i}}{d\beta} = \vec{j}$$
$$\frac{d\vec{j}}{d\beta} = \vec{i} \tag{6}$$

Using obtained partial derivatives in Eq. (6), we can rearrange Eq. (5) as follows

$$\left| \frac{d\vec{\tau}}{d\varphi} = \left(1 + \frac{d\beta}{d\varphi} \right) \right| \tag{7}$$

Referring to Figs. 1 and 2, we conclude from the geometry of fiber, the fiber orientation is expressed as

$$\frac{dx}{dl} = \cos\varphi$$
$$\frac{d\beta}{dx} = \frac{d\theta}{dx}\sin\alpha \tag{8}$$

The value of curvature of the path fiber for the conical shells, by using Eq. (2, 4, 7 and 8), is expressed in the following form

$$\kappa = \frac{d\varphi}{dx}\cos\varphi + \frac{\sin\alpha}{r}\sin\varphi \tag{9}$$

This value depends on the variation of fiber orientation and cone geometry. The geodesic path having zero curvature

$$\frac{d\varphi}{dx}\cos\varphi + \frac{\sin\alpha}{r}\sin\varphi = 0 \tag{10}$$

Employing change of variables $u = r\sin\varphi$, Eq. (10) can be rewritten as follows

$$\frac{du}{dx} = 0 \tag{11}$$

Integration of Eq. (11) yields following expressions

$$r\sin\varphi = r_1\sin\varphi_1 = r_2\sin\varphi_2 = cte \tag{12}$$

And the fiber angle variation for the geodesic path will be

$$\varphi = \arcsin\left(\frac{r_1\sin\varphi_1}{r}\right) \tag{13}$$

Using Eq. (9), the equation for value of curvature of the path fiber for the conical shells with constant curvature κ_c, is expressed in the following form

$$\kappa_c = \frac{d\varphi}{dx}\cos\varphi + \frac{\sin\alpha}{r}\sin\varphi \tag{14}$$

We obtain the fiber angle variation for the constant curvature path in exactly the same way derived in the geodesic path. Fiber angle variation for the constant curvature is

$$\varphi = \arcsin\left(\frac{r_1\sin\varphi_1}{r} + \frac{\kappa_c\left(r^2 - r_1^2\right)}{2r\sin\alpha}\right) \tag{15}$$

Using Eq. (9), the equation for value of curvature of the path fiber for the conical shells with constant angle φ_c, is expressed in the form

$$\kappa = \frac{\sin\alpha}{r}\sin\varphi \tag{16}$$

And the fiber angle variation for the geodesic path can be obtained as follows

$$\varphi = \varphi_c \tag{17}$$

Because the amount of material for unit length of the fiber is constant during the filament winding or the fiber placement process, thickness of the lamina at any point, t is derived as follows

$$t = \frac{t_1 r_1 \cos\varphi_1}{r\cos\varphi} \tag{18}$$

Where, t_1 is the thickness and φ_1 is fiber direction of the lamina at the small edge. Supposing the shell is composed of the angel-ply laminates with N even layers (anti-symmetric) under CST, the corresponding constitutive equations are expressed as follows (Jones 1998)

$$\begin{Bmatrix} N_x \\ N_\theta \\ N_{x\theta} \\ M_x \\ M_\theta \\ M_{x\theta} \end{Bmatrix} = \begin{bmatrix} A_{11} & A_{12} & 0 & 0 & 0 & B_{16} \\ A_{12} & A_{22} & 0 & 0 & 0 & B_{26} \\ 0 & 0 & A_{66} & B_{16} & B_{26} & 0 \\ 0 & 0 & B_{16} & D_{11} & D_{12} & 0 \\ 0 & 0 & B_{26} & D_{12} & D_{22} & 0 \\ B_{16} & B_{26} & 0 & 0 & 0 & D_{66} \end{bmatrix} \begin{Bmatrix} e_x \\ e_\theta \\ e_{x\theta} \\ \kappa_x \\ \kappa_\theta \\ \kappa_{x\theta} \end{Bmatrix} \tag{19}$$
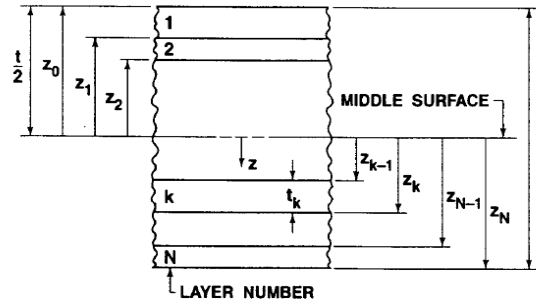
Fig. 3 Geometry of an *N*-layered laminate (Jones 1998)

Where, $N = \{N_x, N_\theta, N_{x\theta}\}^T$ and $M = \{M_x, M_\theta, M_{x\theta}\}^T$ are the internal force and moment resultants vectors, $e = \{e_x, e_\theta, e_{x\theta}\}^T$ and $\kappa = \{\kappa_x, \kappa_\theta, \kappa_{x\theta}\}^T$ are the strain at the reference surface and the change of curvature of the middle surface, respectively, *Aij*, *Bij* and *Dij* (*i, j* = 1, 2, 6) are the membrane, coupling, and flexural stiffness, respectively. These stiffness coefficients can be determined using Eq. (20) (Jones 1998).

$$A_{ij} = \sum_{k=1}^{N} \left(\overline{Q}_{ij}\right)_k \left(Z_k - Z_{k-1}\right)$$

$$B_{ij} = \sum_{k=1}^{N} \left(\overline{Q}_{ij}\right)_k \left(Z_k^2 - Z_{k-1}^2\right)/2 \qquad (20)$$

$$D_{ij} = \sum_{k=1}^{N} \left(\overline{Q}_{ij}\right)_k \left(Z_k^3 - Z_{k-1}^3\right)/3$$

Where, $(\overline{Q}_{ij})_k$ are elastic stiffness constants of the *k*th layer. Z_k and Z_{k-1} are defined in the basic laminate geometry of Fig. 3.

3. Results and discussions

In this section, results in the three sub-section are described. At first, the influence of the fiber paths on the variable ply angle and variable thickness, and then, the influence of the fiber path on stiffness coefficient are presented. Finally, the influence of the fiber paths on the buckling loads is presented.

3.1 Results for the fibers path

In this section, the variable ply angle and variable thickness along the axial coordinate, are presented for an angle-ply laminated conical shell with three different fiber path tailored. The fiber orientation of the ply of TCS versus the normalized longitudinal coordinated for the geodesic path is shown in Fig. 4. The results are in accordance with those results have been derived by Goldfeld *et al*. (2005). The variation of fiber orientation along the longitudinal coordinate for these shells is
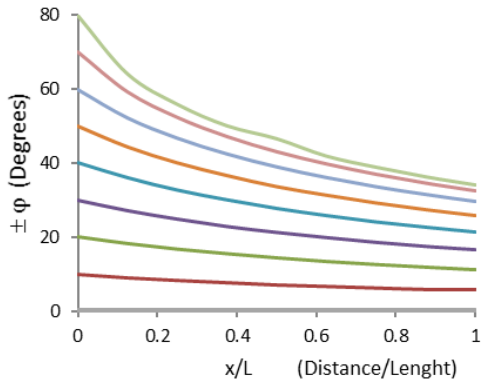
Fig. 4 Fiber orientation for the geodesic TCS
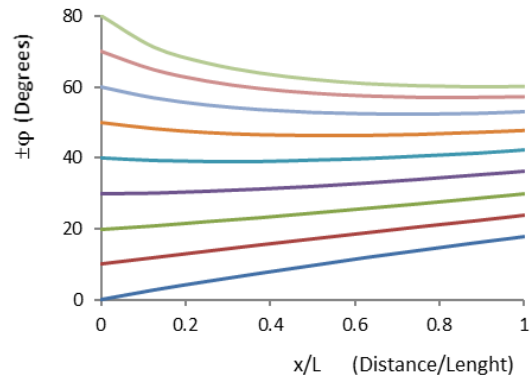
Fig. 5 Fiber orientation for the constant curvature TCS

being higher with higher the ply angle at the small end.

The fiber orientation of the ply for constant curvature path ($\kappa_c = 1.94$ m^{-1}) TCS versus the normalized longitudinal coordinated, shown in Fig. 5. The variation of fiber orientation along the longitudinal coordinate for these shells is being lowest near 40° ply angle at the small end. The angles far than 40° the ply angle at the small end the more rapid the change along the longitudinal coordinate.

In Fig. 6, it is shown that the thickness of each layer at the small end of the conical shell tailored with the fiber on the constant angle path is larger than that at the large end. The results of variation of thickness of each layer versus the longitudinal coordinated conical shell tailored with the geodesic path are presented in Fig. 7. It is seeing that the thickness of each layer at the small end is greater than same parameter at the large end and rate of the variation of shell thickness along the axial direction is increasing with increasing the ply-angle of tailored fiber at small end. These results have a good conformity with the results of Goldfeld *et al.* (2005).
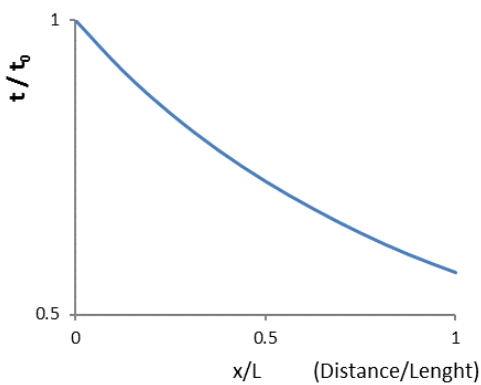
Fig. 6 Normalized thickness for the constant angle TCS
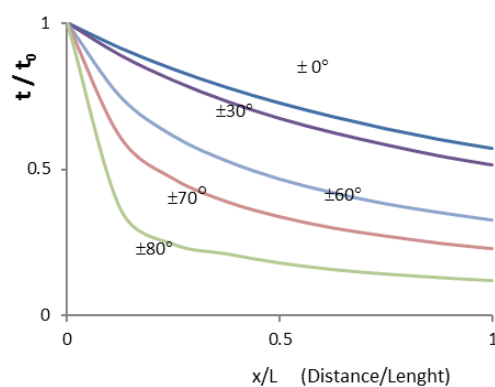
Fig. 7 Normalized thickness for the geodesic TCS
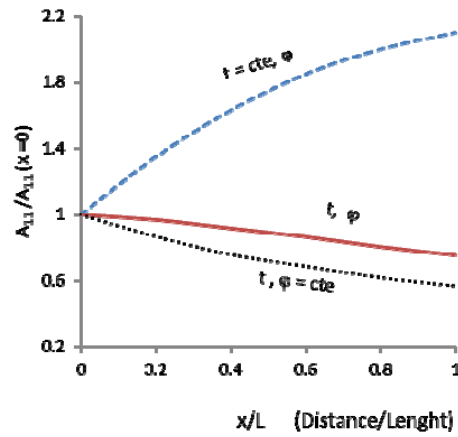
Fig. 8 Normalized stiffness coefficient A_{11} for the geodesic TCS
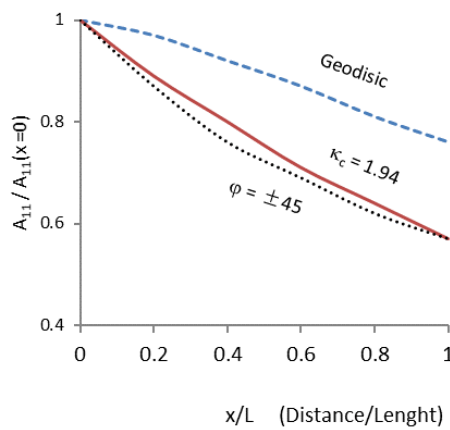
Fig. 9 Normalized stiffness coefficient A_{11} of the TCS

3.2 Results for the stiffness coefficients

In this section, numerical results are presented in order to study the influence of fiber path on stiffness coefficients of an angle-ply laminated conical shell with three different fiber path tailored. The geometric and the material properties are in accordance with related references (Tong and Wang, 1992, Goldfeld *et al.* 2005). The geometrical and material properties of the shell are assumed

$$L = 0.2 \, \text{m}, \quad \alpha = 30°, \quad r_1 = 0.1325 \, \text{m}, \quad t_1 = 1.16 \, \text{mm}$$

$$E_{11} = 97.5 \, \text{GPa}, \quad E_{22} = 8.3 \, \text{GPa}, \quad G_{12} = 4.1 \, \text{GPa}, \quad n_{12} = .32$$

It is assumed that the conical shell is made of CFRP (carbon fiber reinforced plastic).
The stiffness coefficients are computed by a code base on CST. To isolate the influence of the

effects of the variation of thickness and the variation of fiber orientation on the coefficients, each of them was artificially fixed. For sample, the stiffness coefficient A_{11} of those two artificial is plotted in Fig. 8. It is seen that the variation of thickness along the axial direction has significantly more influence on the stiffness coefficients than the variation of fiber orientation along the axial direction.

In Fig. 9 normalized stiffness coefficient A_{11} is plotted versus the longitudinal coordinate for the CTS that they tailored with three paths $[\pm \varphi]$. Three different theoretical path are geodesic path, constant curvature ($\kappa_c = 1.94$) path and constant angle $[\pm 45°]$ path. The stiffness coefficient is affected by the fiber orientation. The stiffness coefficient decreases by approximately 20% for the geodesic tailored and 60% for the tailored constant curvature ($\kappa_c = 1.94$) path and constant angle $[\pm 45°]$ path. The result of the geodesic path is conformed to the result of Goldfeld *et al.* (2005).

For the rest of stiffness coefficients A_{ij}, B_{ij} and D_{ij} the results are as same as A_{11}. The stiffness coefficients are affected by the dependence of thickness, and orientation of fiber in the longitudinal coordinate. In Fig. 10 the normalized stiffness coefficient B_{16} is plotted versus the longitudinal coordinated for three paths of tailored angle-ply $[\pm \varphi]$ laminated conical shell ($\alpha = \pm 30°$, $r_1 = 0.1325$ m and $L = 0.2$ m) with CFRP material. Three different theoretical path are the geodesic path, the constant curvature ($\kappa_c = 1.94$) path and constant angle $[\pm 45°]$ path. The stiffness coefficient is affected by the fiber orientation. The stiffness coefficient decreases approximately 80% for the geodesic tailored and 70% for the tailored constant curvature ($\kappa_c = 1.94$) path, and constant angle $[\pm 45°]$ path. The result of the geodesic path is validated by the result of Goldfeld *et al.* (2005).

In Fig. 11 normalized stiffness coefficient D_{11} is plotted versus the longitudinal coordinated conical shell for three paths tailored angle-ply $[\pm \varphi]$ laminated conical shell ($\alpha = \pm 30°$, $r_1 = 0.1325$ m and $L = 0.2$ m) with CFRP material. Three different theoretical path are the geodesic path, the constant curvature ($\kappa_c = 1.94$) path, and constant angle $[\pm 45°]$ path. The stiffness coefficient is affected by the fiber orientation. The stiffness coefficient decreases approximately 85% for the geodesic tailored and 80% for the tailored constant curvature ($\kappa_c = 1.94$) path, and constant angle $[\pm 45°]$ path. The result of the geodesic path is validated by the result of Goldfeld *et al.* (2005).
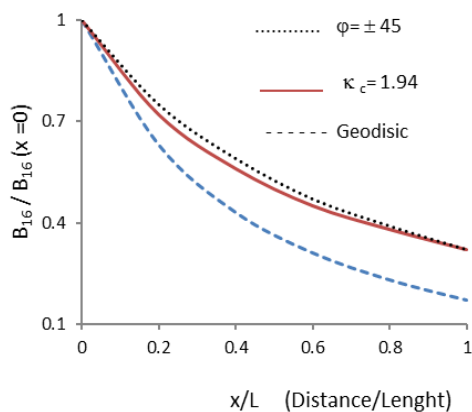
Fig. 10 Normalized stiffness coefficient B_{16} of the TCS
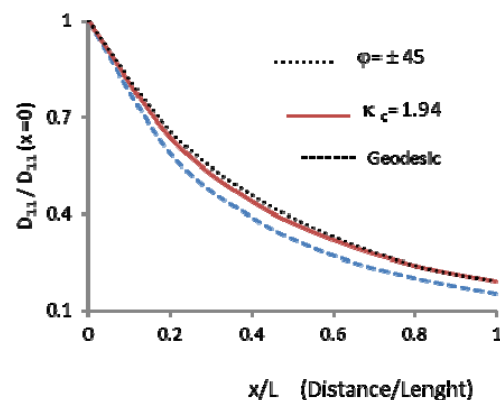
Fig. 11 Normalized stiffness coefficient D_{11} of the TCS

3.3 Results for the buckling analysis

The static and buckling analysis of the conical composite shell is performed using FEA software based on the eigenvalue analysis. Due to varying stiffness of the geodesic and constant curvature path, setting up a finite-element model is more complicated than for the constant angle composite laminates. For the three defined paths, the properties of every element can be
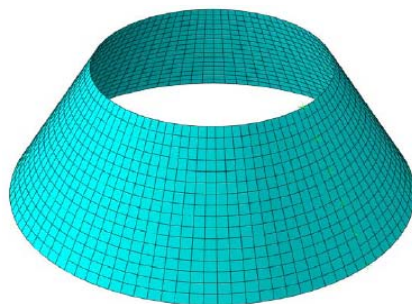
(a) Finite-element model
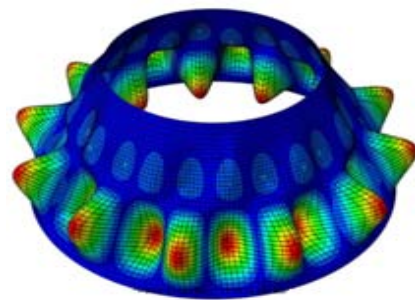
(b) Constant angle and geodesic tailored at the small end [± 0°]
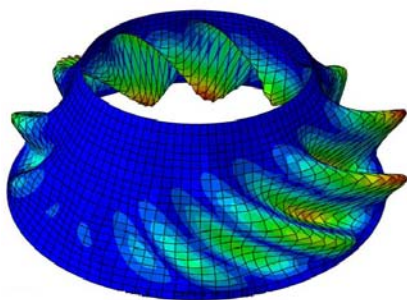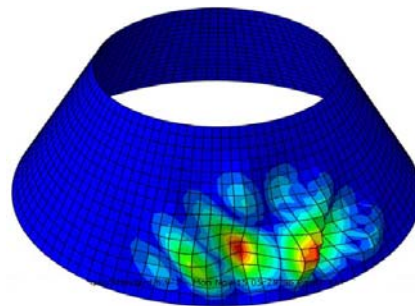
(c) Constant curvature tailored at the small end [± 0°]   (d) Constant angle tailored at the small end [± 45°]
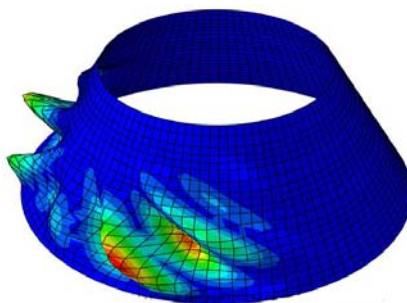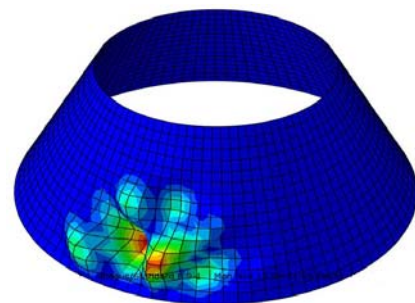
(e) Geodesic tailored at the small end [± 45°]   (f) Constant curvature tailored at the small end [± 45°]

Fig. 12 (a) Finite-element model and (b)-(d) first Buckling mode shapes of TCS for the three paths that ply angel of shells at the small end were [± 0°] and [± 45°] degrees, respectively

considered approximately based on the local stacking sequences of the element. The buckling behavior is extremely depends on the stiffness coefficients. In this work, based on Goldfeld *et al*. (2005), the buckling load and the buckling mode are calculated by the ABAQUS software. The stiffness matrices are calculated at each mesh-point. Buckling analysis of the conical composite shell is performed using FEA by the ABAQUS software. Finite-element modeling of the TCS is carried out with eight node element where for each node, three translation degree of freedom and three rotational degrees of freedom along the nodal direction (Fig. 12(a)).

The main objective of this study is to investigate the influence of the fiber path on the buckling behavior of the TCS. The buckling load was computed by the inclusion of variation of stiffness coefficients. This was done by calculation of stiffness coefficients for each fiber path TCS by a subroutine, and the buckling load was computed by ABAQUS software. The buckling mode shape of conical shell tailored with fiber path ([± φ]) by finite-element modeling (ABAQUS software) is given in Fig. 12. One can see that not only is the buckling load different, but the buckling mode is too.
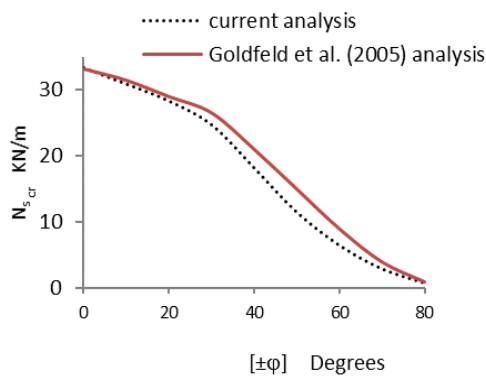
Fig. 13 Normalized buckling load versus the ply orientation at the small end of the geodesic TCS
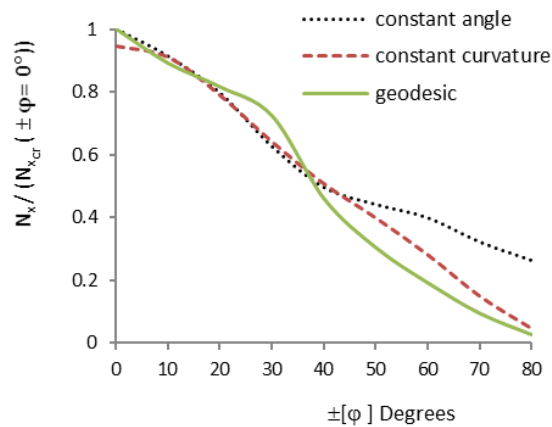
Fig. 14 Normalized buckling load of TCS for three paths

The buckling load is affected by the dependence of thickness, and the orientation of fiber on the longitudinal coordinate. In Fig. 13 the buckling load current and Goldfeld *et al.* (2005) plotted again the fiber's inclination at the small end of the shell for the geodesic TCS (filament winding process) ($\alpha = \pm 30°$, $r_1 = 0.1325$ m and $L = 0.2$ m) under axial load with CFRP material. The higher ply angle at the small end leads to the lower the thickness and it leads to lower buckling load. The results are showing a good conformity with results of Goldfeld *et al.* (2005).

Shown in Fig. 14 are the buckling loads in terms of the fiber's inclination at the small end of the shells. TCS ($\alpha = \pm 30°$, $r_1 = 0.1325$ m and $L = 0.2$ m) of CFRP material are under axial load. It is seen that for the shells being tailored with three paths (the geodesic path, the constant curvature path, and constant angle path), as the ply angle at the small end of the shell increases, the thickness of the shell decreases which leads to lower buckling load. The higher ply angle at the small end leads to the more rapid decrease of the buckling load. Shells that being tailored with angles more than $\pm 45°$ on constant angle path were exceptional cases, so the buckling load decreases moderately with increasing the ply angle at the small end of shell.

4. Conclusions

In this study, the stiffness of the tailored composite conical shells was investigated for three fiber orientations were containing constant angle path, the geodesic path or the constant curvature path. The obtained results indicate that the stiffness coefficients based on the path fiber and ply orientation at the start of tailored are variable, and they are functions of the shell coordinates. Furthermore, the buckling loads based on the path fiber and ply orientation at the start of tailored fiber gets to be different. The extent of difference in the start angle of the tailored fiber lower than 20 degrees is not significant. It can be concluded that the buckling load is generally most affected by the rate of decreasing of the thickness along the axial direction. When the start angle of the tailored fiber at the small end of the shell gets to be larger value, the thickness along longitudinal coordinate of the cone reduces very rapidly, which lead to rapidly the reduction of the stiffness and the buckling load.

References

Abdalla, M.M., Setoodeh, S. and Gurdal, Z. (2007), "Design of variable stiffness composite panels for maximum fundamental eigenfrequency using lamination parameters", *Comput. Struct.*, **81**(2), 283-291.

Arbocz, J. (1968), Buckling of conical Shells under axial compression, NASA, Report CR-1162.

Baruch, M., Arbocz, J. and Zhang, G.Q. (1993), "Laminated conical shells consideration for the variations of the stiffness coefficients", *Proceeding of the* 35*th AIAA/ASME/ASCE/AHS/ASC S.S.D.M. Conference*, Hilton Head, SC, USA.

Baruch, M., Harai, O. and Singer, J. (1970), "Low buckling of axially compressed conical shells", *J. Appl. Mech.*, **37**(2), 384-392.

Blom, A.W., Abdalla, M.M. and Gurdal, Z. (2010), "Optimization of course locations in fiber-placed panels for general fiber angle distributions", *Compos. Sci. Technol.*, **70**(4), 564-570.

Blom, A.W., Setoodeh, S., Hol, J.M.A.M. and Gurdal, Z. (2008), "Design of variable-stiffness conical shells for maximum fundamental eigenfrequency", *Comput. Struct.*, **86**(9), 870-878.

Blom, A.W., Tatting, B.F., Hol, J.M.A.M. and Gurdal, Z. (2009), "Fiber path definitions for elastically tailored conical shells", *Compos. Part B. Eng.*, **40**(1), 77-84.

Goldfeld, Y. (2007a), "Imperfection sensitivity of laminated conical shells", *Int. J. Solid. Struct.*, **44**(3-4),

1221-1241.

Goldfeld, Y. (2007b), "Elastic buckling and imperfection sensitivity of generally stiffened conical shells", *AIAA J.*, **45**(3), 721-729.

Goldfeld, Y. and Arbocz, J. (2004), "Buckling of laminated conical Shells given the variation of the stiffness coefficients", *AIAA J.*, **42**(3), 642-649.

Goldfeld, Y., Arbocz, J. and Rothwell, A. (2005), "Design and optimization of laminated conical shells for buckling", *Thin-Wall. Struct.*, **43**(1), 107-133.

Jones, R.M. (1998), *Mechanics of Composite Materials*, Taylor & Francis, London, UK.

Seide, P. (1956), "Axisymmetrical buckling of circular cones under axial compression", *J. Appl. Mech.*, **23**, 626-628.

Seide, P. (1957), "A donnell-type theory for asymmetrical bending and buckling of thin conical shells", *J. Appl. Mech.*, **24**, 547-552.

Singer, J. (1963), "Donnell-type equations for bending and buckling of orthotropic conical shells", *ASME J. Appl. Mech.*, **30**(2), 303-305.

Tong, L. (1998), "Buckling of filament wound composite conical shells under axial compression", *AIAA J.*, **37**(6), 779-781.

Tong, L. and Wang, T.K. (1992), "Simple solutions for buckling of laminated conical shells", *Int. J. Mech. Sci.*, **34**(2), 93-111.

Tong, L., Tabarrok, B. and Wang, T.K. (1992), "Simple solution for buckling of orthotropic conical shells", *Int. J. Solid Struct.*, **29**(8), 933-946.

CC